Chemical Engineering Journal 162 (2010) 43–50

Contents lists available at ScienceDirect

Chemical Engineering Journal

journal homepage: www.elsevier.com/locate/cej

NaOH-activated carbon from flamboyant (*Delonix regia*) pods: Optimization of preparation conditions using central composite rotatable design

Alexandro M.M. Vargas[a], Clarice A. Garcia[b], Edson M. Reis[a], Ervim Lenzi[a], Willian F. Costa[a], Vitor C. Almeida[a,*]

[a] Department of Chemistry, Universidade Estadual de Maringá, Av. Colombo 5790, CEP 87020-900 Maringá, Paraná, Brazil
[b] Department of Chemical Engineering, Universidade Estadual de Maringá, Av. Colombo 5790, CEP 87020-900 Maringá, Paraná, Brazil

ARTICLE INFO

Article history:
Received 13 March 2010
Received in revised form 27 April 2010
Accepted 28 April 2010

Keywords:
Activated carbon
Response surface methodology
Optimization
Chemical activation
Microporosity

ABSTRACT

The conditions for the preparation of activated carbon from flamboyant pods treated with NaOH were optimized through response surface methodology (RSM) and central composite rotatable design (CCRD). The effects of the activation temperature, activation time, and impregnation ratio were studied from the BET surface area, micropore volume, and yield results. The results showed that the activation temperature and the impregnation ratio are the factors that most influence the activated carbon production. Activation temperature of 761.70 °C, activation time of 0.86 h, and impregnation ratio (NaOH:char) of 3.46 led to BET surface area, micropore volume, and yield values of 2854 $m^2 g^{-1}$, 1.44 $cm^3 g^{-1}$, and 10.80%, respectively. Porosity parameters and scanning electron microscopy were used to investigate the activated carbon obtained under optimal conditions.

1. Introduction

The constant concern with the increase in the quantity of pollutant gases released into the atmosphere has led to the search for materials capable of capturing these gases and reducing their environmental impact. Microporous activated carbons (ACs) are some of the most appropriate porous materials for the removal of gases and have applications in the most varied areas [1].

Chemical activation using bases (KOH or NaOH) is one of the most efficient methods of production of microporous ACs with large surface areas [2–4]. The two-step chemical activation has raised much interest due to the good results obtained as compared to one-step activation [5]. In this process, an initial carbonization step produces a material free of volatile compounds, and the second step (activation) allows the development of porosity.

Various precursors, both of mineral and of vegetable are used in the production of ACs. Researchers have reported the preparation of chemically ACs from many kinds of raw materials, such as coconut husks [6,7], Spanish anthracite [3], olive husk [8], sewage sludge [9], petroleum coke [10], Siberian anthracite [2], coffee endocarp [11], cotton stalks [12], plum kernels [13], coal tar pitch [4], fir wood and pistachio shells [14,15], and olive stones [16]. Besides being renewable resources, biomasses are inexpensive, largely available, have low ash contents, a greater diversity, and a short production time.

The most studied chemical activation parameters are time, temperature, and impregnation ratio (activating agent:char). In most studies, one factor is fixed at a certain level, varying another to determine the best condition. This procedure has disadvantages such as: (i) the lack of research on the interactive effects of the studied factors, and (ii) the large number of experiments required, which consequently require more time with a higher cost and consumption of reagents [17].

Multivariate statistical techniques arise as an important tool for the optimization of analytical procedures. One of the most important multivariate techniques used in optimization analysis is response surface methodology (RSM) [18]. This method consists of diverse mathematical and statistical techniques based on the adjustment of a polynomial equation and symmetrical models to the experiment data to describe the behavior of the independent variables [17]. Among the second-order symmetrical models most used in analytical procedures, central composite rotatable design (CCRD) has been widely applied in various scientific areas [19]. In recent years, some authors have applied this optimization method to the production of ACs [6,7,20,21].

Delonix regia, a flowering tree species from the Fabaceae family, is known for its fern-like leaves and flamboyant display of flowers. It grows in southern Brazil and is also found in other parts of the world. The pods gradually fall off the trees after a period of maturation. Due to their abundance and lack of use, the pods

* Corresponding author. Tel.: +55 44 3261 3678; fax: +55 44 3261 4334.
E-mail address: vcalmeida@uem.br (V.C. Almeida).

1385-8947/$ – see front matter © 2010 Elsevier B.V. All rights reserved.
doi:10.1016/j.cej.2010.04.052

may be a very interesting precursor for the production of low-cost ACs.

The main objective of this study was to apply CCRD to optimize the production of ACs from flamboyant pods chemically activated with NaOH. The AC obtained in optimized conditions (AC_{op}) was investigated through analyses of the porosity parameters and scanning electron microscopy (SEM).

2. Methods

2.1. Raw material

Flamboyant pods for the production of ACs were collected from trees located in the region of Maringá City, Paraná, Brazil. The proximate analysis of the study raw material using ASTM D1762-84 Standards [22] gave moisture, ash, volatile matter, and fixed carbon contents of 5.98, 2.16, 61.20, and 30.66%, respectively.

2.2. Preparation of NaOH-activated carbons

Flamboyant pods were washed with distilled water and dried at 110 °C for 24 h. The material, which had particle sizes between 250 and 425 μm, was placed in a horizontal stainless steel reactor and heated in a furnace at a rate of 20 °C min^{-1} from room temperature to 500 °C and maintained at this temperature for 1.5 h under N_2 flow of 100 cm^3 min^{-1}. The char produced from the carbonization process was mixed with varying amounts of sodium hydroxide pellets (Merck, Germany) at different impregnation ratios (NaOH:char) in a vertical stainless steel reactor under magnetic stirring for 2 h, and then dried at 130 °C for 4 h. The reactor containing the dry mixture was placed into a furnace under N_2 flow of 100 cm^3 min^{-1}, heated at a rate of 20 °C min^{-1} up to the desired final temperature for defined times. After cooling, the resulting mixture was washed with a solution of 0.1 mol L^{-1} HCl, followed by hot distilled water until pH ~6.5. The carbon was separated using 0.45-μm membrane filters, dried at 110 °C for 24 h, and kept in tightly closed bottles for further analysis.

2.3. Experimental design for the response surface procedure

RSM and CCRD were applied to determine the best combination of activation process factors: activation temperature (°C), activation time (h), and impregnation ratio (NaOH:char). The experimental planning responses were the BET surface area (S_{BET}), micropore volume (V_μ), and yield.

The CCRD is a very efficient design for fitting the second-order model. In this planning, it is common to codify the variable levels, generally assuming three equally spaced levels, −1, 0, and +1 for low, intermediate, and high values, respectively [17]. This level codification consists of transforming each real value into a coordinate within a dimensional value scale proportional to their location in the experimental space or their distance from the center [19]. The coded values of each factor level were obtained by Eq. (1):

$$x_i = \frac{X_i - X_0}{\Delta X_i} \quad (1)$$

where x_i is the coded value for each factor, X_i is the real value for each factor, X_0 is the real value for each factor at the central point, and ΔX_i is the difference between the levels of each factor. The experiment data were adjusted to a second-order polynomial regression model, expressed by Eq. (2):

$$Y = \beta_0 + \sum_{i=1}^{3} \beta_i x_i + \sum_{i=1}^{3} \beta_{ii} x_i^2 + \sum_{i=1}^{2} \sum_{j=i+1}^{3} \beta_{ij} x_i x_j \quad (2)$$

where β_0, β_i, β_{ii}, and β_{ij} are the regression coefficients (β_0 is the constant term, β_i is the linear effect term, β_{ii} is the quadratic effect term, and β_{ij} is the interaction effect term), and Y is the response value predicted by the model.

A central composite design is made rotatable by the choice of "α". The term "α" represents the planning rotatability and depends on the number of factors used, as, for example, 1.41, 1.68, and 2 for two, three, and four factors, respectively [18].

Variance analyses (ANOVA) were carried out in order to determine the statistical significance of the models, the factors or coefficients, and of the residues. The fitting quality of the polynomial model was evaluated by way of the determination coefficient (R^2). The program STATISTICA 7.0 (StatSoft) was used to develop and analyze all the parameters and experiment data.

2.4. Textural and chemical analysis

Textural properties were deduced from nitrogen adsorption at 77 K (QuantaChrome Nova1200 surface area analyzer). The BET surface area, S_{BET}, was determined from the isotherms using the Brunauer–Emmett–Teller equation (BET). The total pore volume, V_T, was defined as the volume of liquid nitrogen corresponding to the amount adsorbed at a relative pressure of $P/P^0 = 0.99$ [23]. The micropore volume, V_μ, was determined with the Dubinin–Radushkevich equation [23], and the mesopore volume, V_m, was calculated as the difference between V_T and V_μ. The pore diameter, D_p, was calculated using the ratio $4\,V_T/S_{BET}$, and the pore size distribution, by the HK method [24].

The AC yield was defined as the final weight of the product after activation, washing, and drying. The percent yield was determined from Eq. (3):

$$\text{Yield} = \left(\frac{w_c}{w_0}\right) \times 100 \quad (3)$$

where w_c and w_0 are the dry mass values of the final AC (g) and the precursor (g), respectively.

The morphology of the raw material and AC_{op} was examined by scanning electron microscopy (Shimadzu, model SS 550).

3. Results and discussion

3.1. RSM experiments and model fitting

Generally, the CCRD consists of a 2^k factorial runs with $2k$ axial runs and n_c center runs, where k is the number of factors. The CCRD consisted of eight factorial points or cubic points, six axial points or star points (two axial points on each variable axis at a distance ("α") of 1.68 from the center), and 4 replicates at the central point, for a total of 18 experiments. The four replicates at the central point were used to determine the pure error and the variance. The real and codified values of the three factors of each experiment are shown in Table 1. The development of the experiments as well as the experimental response values of S_{BET}, V_μ, and yield is shown in Table 2.

Table 1
Coded and actual levels for independent factors used in the experimental design.

Factors	Coded values				
	$-\alpha(-1.68)$	−1	0	+1	$+\alpha(+1.68)$
	Actual values				
Activation temperature (°C), X_1	531.82	600	700	800	868.18
Activation time (h), X_2	0.66	1	1.5	2	2.34
Impregnation ratio (NaOH:char), X_3	0.32	1	2	3	3.68

Table 2
Central composite rotatable design of three factors and five levels.

Order	X_1[a] (x_1)[b]	X_2[a] (x_2)[b]	X_3[a] (x_3)[b]	S_{BET} ($m^2\ g^{-1}$)	V_μ ($cm^3\ g^{-1}$)	Yield (%)
1	600 (−1)	1 (−1)	1 (−1)	360.9	0.181	20.59
5	800 (+1)	1 (−1)	1 (−1)	711.7	0.353	14.64
7	600 (−1)	2 (+1)	1 (−1)	305.6	0.157	18.98
3	800 (+1)	2 (+1)	1 (−1)	794.2	0.398	13.92
4	600 (−1)	1 (−1)	3 (+1)	1664	0.838	13.58
8	800 (+1)	1 (−1)	3 (+1)	2372	1.161	10.75
16	600 (−1)	2 (+1)	3 (+1)	2146	1.088	11.59
6	800 (+1)	2 (+1)	3 (+1)	2351	1.148	11.25
10	531.82 (−1.68)	1.5 (0)	2 (0)	1076	0.550	16.79
11	868.18 (+1.68)	1.5 (0)	2 (0)	1850	0.935	9.78
15	700 (0)	0.66 (−1.68)	2 (0)	1388	0.684	15.44
17	700 (0)	2.34 (+1.68)	2 (0)	1400	0.687	13.73
12	700 (0)	1.5 (0)	0.32 (−1.68)	409.1	0.204	15.8
9	700 (0)	1.5 (0)	3.68 (+1.68)	3124	1.531	9.66
2	700 (0)	1.5 (0)	2 (0)	1650	0.828	13.91
18	700 (0)	1.5 (0)	2 (0)	1549	0.762	15.05
13	700 (0)	1.5 (0)	2 (0)	1702	0.868	14.63
14	700 (0)	1.5 (0)	2 (0)	1732	0.877	13.34

S_{BET} = BET surface area, V_μ = micropore volume.
[a] Actual values.
[b] Coded values.

Each experiment was performed in triplicate and the average values were used. For statistical reasons, the experiments were carried out in a random order to avoid bias errors.

The significance of regression was evaluated by the ratio between the media of the square of regression and the media of the square of residuals and by comparing these variation sources using the F distribution ($F = 0.05$), taking into account its respective degrees of freedom associated to regression and to residual variances. Thus, a statistically significant value for this ratio must be higher than the tabulated value. The lack of fit was evaluated by the ratio between the media of the square due to lack of fit and the media of the square due to pure error and by comparing these variation sources using the F distribution ($F = 0.05$) taking into account its respective degrees of freedom associated with the lack of fit and the pure error variances. If this ratio is higher than the tabulated value, it is concluded that there is evidence of a lack of fit and that the model needs to be improved. However, if the value is lower than the tabulated value, the model fitness can be considered satisfactory [19].

The p value also was used to evaluate the significance of the parameters. The lower the p value, the less likely the result, assuming the null hypothesis, the more significant the result, in the sense of statistical significance [17]. One often rejects a null hypothesis if the p value is less than 0.05, corresponding to a 5% chance of an outcome at least that extreme, given the null hypothesis.

3.1.1. BET surface area and micropore volume

Table 3 presents the variance analysis of all of the linear, quadratic, and interaction effects of the three planning factors with regard to S_{BET} and V_μ. The x_1, x_3, $(x_1)^2$, and $(x_2)^2$ effects are significant for the S_{BET}, and on the other hand, the x_2, $(x_3)^2$, x_1x_2, x_1x_3, and x_2x_3 effects are not significant. The x_1, x_3, and $(x_2)^2$ effects are significant for the V_μ, and the x_2, $(x_1)^2$, $(x_3)^2$, x_1x_2, x_1x_3, and x_2x_3 effects are not significant.

A quadratic regression model was obtained for S_{BET} and V_μ. The codified values for the quadratic equation after excluding the insignificant terms are shown in Eqs. (4) and (5):

$$S_{BET} = 1667.73 + 223.63x_1 + 800.07x_3 - 111.45(x_1)^2 - 135.84(x_2)^2 \quad (4)$$

$$V_\mu = 0.84 + 0.11x_1 + 0.39x_3 - 0.073(x_2)^2 \quad (5)$$

The quadratic regression equation shows that the significant terms present different characteristics. The elevated values of terms x_1, x_3, $(x_1)^2$, and $(x_2)^2$, in relation to the other terms, indicate that they have a greater importance or influence. Positive values indicate that the terms increase the response and the negative values decrease the response. The linear effects of the ratio NaOH:char (x_3) and the temperature (x_1) present high and positive values, indicating that the increase in these terms increases the surface area and micropore volume in the studied experiment region. The term x_3 is much greater than x_1, indicating that the ratio NaOH:char is the most important among the response factors. However, the quadratic effects of temperature $(x_1)^2$ (for S_{BET}) and time $(x_2)^2$ (for S_{BET} and V_μ) were significant and negative, showing that the increase in temperature and time beyond the studied experiment region tends to decrease the surface area and micropore volume. The interaction effects were not significant.

3.1.2. Yield

The variance analysis for all three factor effects (linear, quadratic, and interaction) for the yield is shown in Table 3. The x_1, x_3, and x_1x_3 effects are significant, and the x_2, $(x_1)^2$, $(x_2)^2$, $(x_3)^2$, x_1x_2, and x_2x_3 effects are not significant. A quadratic regression model was obtained for the yield. The codified values of the quadratic equation after excluding the insignificant terms are shown in Eq. (6):

$$\text{Yield} = 14.19 - 1.90x_1 - 2.29x_3 + 0.98x_1x_3 \quad (6)$$

The linear temperature terms (x_1) and the ratio NaOH:char (x_3) exert a negative influence on the response. The temperature increase and the NaOH:char ratio cause a decrease in the yield. The interaction term x_1x_3 is significant and has a positive signal; however, it has little influence on the yield. Therefore, the impregnation ratio has a greater influence on the yield.

3.2. Variance analyses (ANOVA) of the models

Table 4 shows the variance analysis (ANOVA) of the quadratic model adjusted to S_{BET}, V_μ, and yield. For S_{BET}, the regression model presents an F ratio of 42.63, which is higher than the tabulated value of $F = 0.05_{(9,8)} = 3.39$. The regression p value obtained (<0.0001) is less than the value of 0.05. Therefore, according to the F ratio and p value, the quadratic model adjusted for S_{BET} is significant. Additionally, the lack of fit presents an F ratio and p value

Table 3
Variance analyses (ANOVA) for three factors (x_1, x_2, x_3) and S_{BET}, V_μ, and yield results.

Parameter	Sum of squares			Mean square			*F* ratio			*p* value		
	S_{BET}	V_μ	Yield	S_{BET}	V_μ	Yield	S_{BET}	V_μ	Yield	S_{BET}	V_μ	Yield
x_1	6.830×10^5	0.15	49.38	6.830×10^5	0.15	49.38	26.66	22.15	55.07	0.0009	0.0015	<0.0001
x_2	18924.69	5.067×10^{-3}	3.28	18924.69	5.067×10^{-3}	3.28	0.74	0.74	3.66	0.4151	0.4161	0.0920
x_3	8.742×10^6	2.12	71.67	8.742×10^6	2.12	71.67	341.21	307.40	79.93	<0.0001	<0.0001	<0.0001
$(x_1)^2$	1.571×10^5	0.035	0.23	1.571×10^5	0.035	0.23	6.13	5.15	0.26	0.0383	0.0530	0.6247
$(x_2)^2$	2.334×10^5	0.068	1.33	2.334×10^5	0.068	1.33	9.11	9.81	1.48	0.0166	0.0140	0.2581
$(x_3)^2$	215.54	9.677×10^{-4}	1.39	215.54	9.677×10^{-4}	1.39	8.413×10^{-3}	0.14	1.55	0.9292	0.7176	0.2481
x_1x_2	16671.38	4.704×10^{-3}	1.43	16671.38	4.704×10^{-3}	1.43	0.65	0.68	1.59	0.4432	0.4325	0.2425
x_1x_3	677.12	1.125×10^{-4}	7.68	677.12	1.125×10^{-4}	7.68	0.026	0.016	8.57	0.8749	0.9015	0.0191
x_2x_3	23522.80	5.832×10^{-3}	0.088	23522.80	5.832×10^{-3}	0.088	0.92	0.85	0.098	0.3660	0.3844	0.7618

S_{BET} = BET surface area, V_μ = micropore volume, degree of freedom = 1 for all parameters ($x_1, x_2, x_3, x_1^2, x_2^2, x_3^2, x_1x_2, x_1x_3, x_2x_3$).

of 5.75 and 0.0903, respectively. The *F* ratio is less than the tabulated value ($F = 0.05_{(5,3)} = 9.01$) and the *p* value is higher than 0.05, indicating that the lack of fit is insignificant. The determination coefficient (R^2) value of 0.9800 indicates that the regression model explain 98.00% of variations around the average, leaving 2% for the residues.

For V_μ, the regression model presents an *F* ratio and *p* value of 38.30 and <0.0001, respectively; and lack of fit presents an *F* ratio and *p* value of 3.42 and 0.1702, respectively. This is an indication that the mathematical model is well fitted to the experimental data. The determination coefficient (R^2) for this model was 0.9773.

With regard to the yield, the regression model *F* ratio and *p* value were 17.00 and 0.0003, respectively. The lack of fit presents an *F* ratio of 1.89 and a *p* value of 0.3180. Comparing these values with tabulated values for the regression model ($F = 0.05_{(9,8)} = 3.39$) and the lack of fit ($F = 0.05_{(5,3)} = 9.01$), the model is significant and the lack of fit is not significant. The *p* value for the regression model

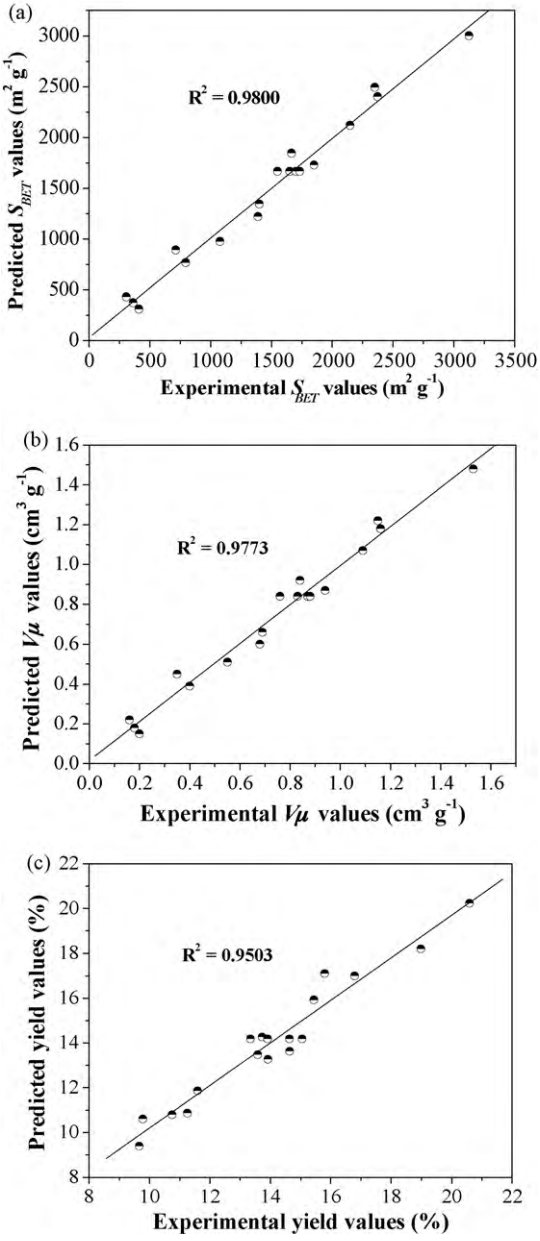

Fig. 1. Relationship between the predicted and the observed values of BET surface area (a), micropore volume (b), and yield (c).

Table 4
Variance analyses (ANOVA) of the quadratic models adjusted to the S_{BET}, V_{μ}, and yield results.

Source	Sum of squares	DF	Mean square	*F* ratio	*p* value	R^2
S_{BET}						
Model	9.830×10^6	9	1.092×10^6	42.63	<0.0001	0.9800
Residual	2.050×10^5	8	25620.86			
Lack of fit	1.856×10^5	5	37122.03	5.75	0.0903	
Pure error	19356.75	3	6452.25			
Total	1.003×10^7	17				
V_{μ}						
Model	2.37	9	0.26	38.30	<0.0001	0.9773
Residual	0.055	8	6.889×10^{-3}			
Lack of fit	0.047	5	9.377×10^{-3}	3.42	0.1702	
Pure error	8.225×10^{-3}	3	2.742×10^{-3}			
Total	2.43	17				
Yield						
Model	137.22	9	15.25	17.00	0.0003	0.9503
Residual	7.17	8	0.90			
Lack of fit	5.45	5	1.09	1.89	0.3180	
Pure error	1.73	3	0.58			
Total	144.40	17				

S_{BET} = BET surface area, V_{μ} = micropore volume, DF = degree of freedom, R^2 = determination coefficient.

and lack of fit are in agreement with the previous description. The determination coefficient (R^2) for this model was 0.9503. Fig. 1a–c shows relationship between the values predicted by the model and the experimental values for the three CCRD responses.

3.3. Analysis of the influence of the factors on the responses

3.3.1. Effect of the activation factors on the BET surface area and micropore volume

Adequate pore development during the activation process leads to ACs with large surface areas. Figs. 2 and 3 show the three-dimensional response surface plots for S_{BET} and V_{μ}, respectively, as a function of two factors, maintaining a third one at its central level. Figs. 2a and b and 3a and 3b describe the effect of the temperature on S_{BET} and V_{μ}, respectively. According to the figures, in the studied range, the surface area and micropore volume increase with temperature. The temperature increase raises reaction rates between the char and NaOH, leading to the development of the porous structure due to the formation and opening of the pores.

The effect of activation time on S_{BET} and V_{μ} is described in Figs. 2a and c and 3a and 3c, respectively. According to the graph, for the conditions studied, time does not significantly influence the development of the AC porosity. Temperatures and activation times outside of the pre-established experimental range may lead to a decrease in the surface area.

The surface area and micropore volume are directly related to the increase in the impregnation ratio (Figs. 2b and c and 3b and 3c). The greater quantity of NaOH in the medium favored the reaction with the char and contributed to increase the surface area and micropore volume. The stoichiometric reaction between NaOH and char during chemical activation can be expressed by Eq. (7) [3,13]:

$$6NaOH + 2C \leftrightarrows 2Na + 2Na_2CO_3 + 3H_2 \quad (7)$$

According to Eq. (7), the stoichiometric ratio of the activating reagent and the char is 3:1, which indicates the need to use a greater quantity of NaOH to form the products. The metallic sodium produced can insert itself into the carbon structure produced and aid in the development of porosity [3]. In this way, large surface areas can be obtained when high impregnation ratios are used. In this study, a S_{BET} of 3124 $m^2\ g^{-1}$ and V_{μ} of 1.531 $cm^3\ g^{-1}$ were obtained at a NaOH:char ratio of 3.68. A similar behavior was observed by El-Hendawy et al. [12], Nowicki et al. [2], and Tseng [13].

3.3.2. Effect of the activation factors on the yield

Fig. 4 shows the three-dimensional response surface plots for the yield as a function of two factors, maintaining a third one at its central level. The effects of temperature and impregnation ratio significantly influenced the yield response. The temperature increase (Fig. 4a and b) favors the direct reaction described by Eq. (7), which generates a greater consumption of char and a consequent decrease in the yield.

The effect of the impregnation ratio on the yield was similar, but more pronounced than that of the activation temperature (Fig. 4a and c). The aggressive attack of the base on the char causes its degradation through oxidation and elimination reactions, leading to the breaking of the C–O–C and C–C bonds, which causes its structure to disintegrate [5]. The results are in accordance with the work carried out by Nowicki et al. [2], Wu et al. [14], and Mácia-Agulló et al. [4].

Fig. 4b and c shows the possible effect of the time factor on the yield of the ACs. According to the graphs, activation time did not influence the yield values. Therefore, high yield values were obtained when the three factors were maintained at the minimum interval level of the studied values.

3.4. Optimization process

The optimal response values and real factor values that provided these responses were obtained using the simultaneous optimization technique proposed by Derringer and Suich [25]. This method is based on the definition of a desirability function (d) for each response, with values restricted to the interval $0 \leq d \leq 1$, where if the response is at its goal or target, then $d = 1$, and if the response is outside an acceptable region, $d = 0$ [18]. The objective of the optimization of the AC production was to find factor values which provided the greatest yield, S_{BET}, and V_{μ} results. However, the optimization of these results is difficult, because the factors region of interest is different, that is, S_{BET} and V_{μ} show an inverse correlation with yield. This being the case, S_{BET} (305.6–3124 $m^2\ g^{-1}$) and V_{μ} (0.157–1.531 $cm^3\ g^{-1}$) were maximized in the values within the experiment domain and the yield was maintained in the value range between 10 and 15%. In optimal conditions, a desirability value $d = 0.89$ was obtained with the program STATISTICA 7.0 (StatSoft). Optimal ACs were obtained under the following production conditions: activation temperature of 761.70 °C, activation time of 0.86 h, and impregnation ratio (NaOH:char) of 3.46. Table 5 shows the modeling and the experimental values obtained in the aforementioned conditions. The differences between the surface area,

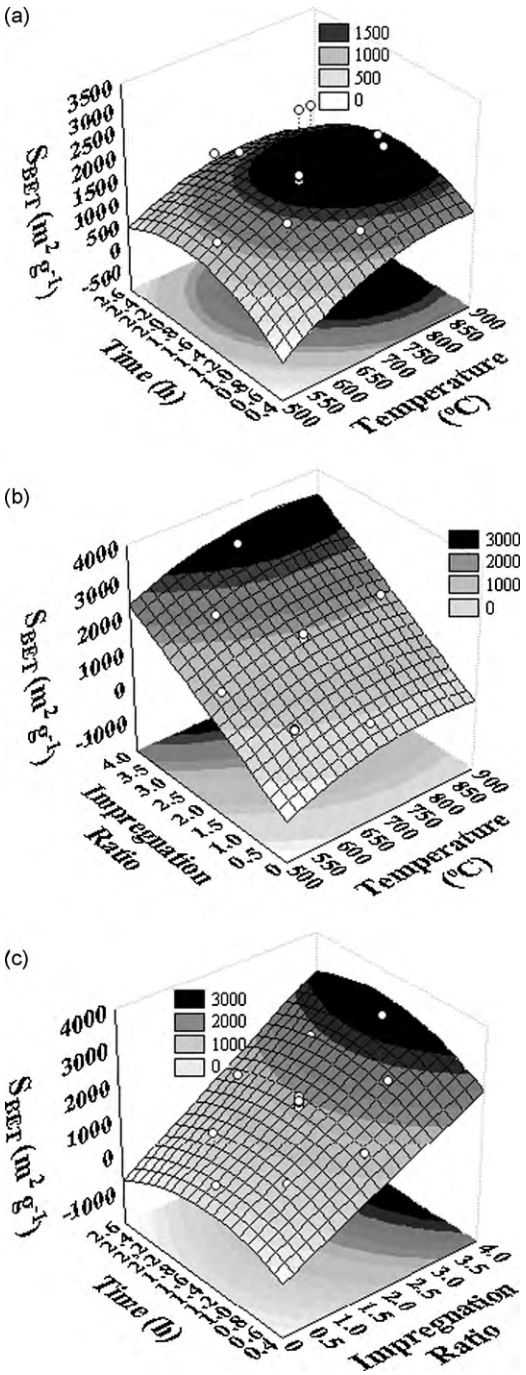

Fig. 2. Three-dimensional response surface plots for BET surface area: temperature and time (a), temperature and impregnation ratio (b), and impregnation ratio and time (c).

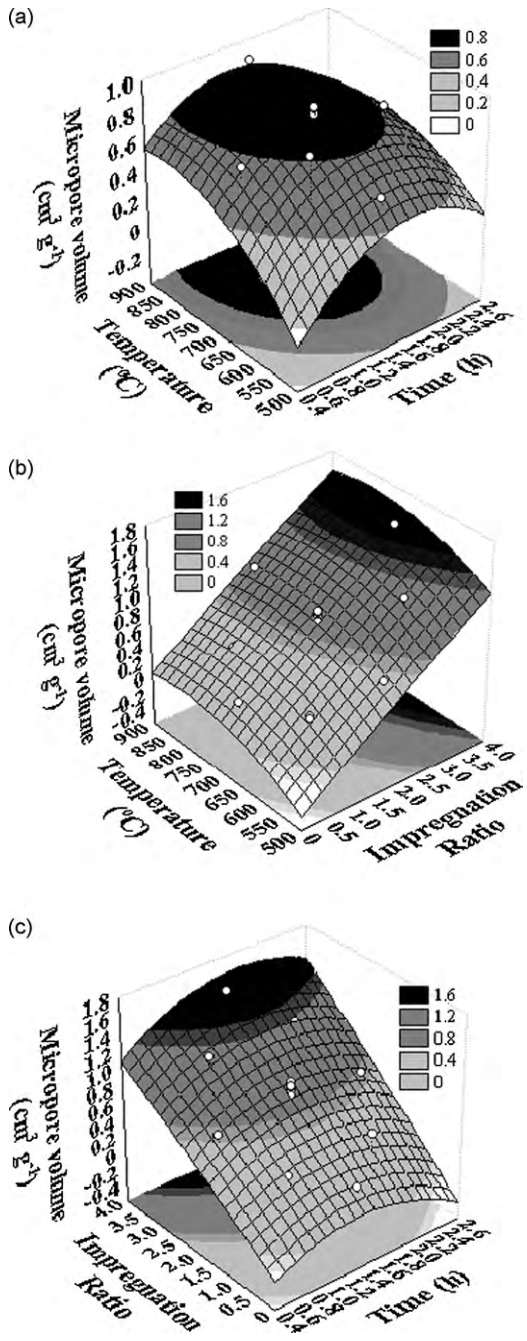

Fig. 3. Three-dimensional response surface plots for micropore volume: time and temperature (a), impregnation ratio and temperature (b), time and impregnation ratio (c).

micropore volume, and yield values predicted by the model and the experimental values were 6.88, 8.87, and 2.46%, respectively. The difference in the values with regard to the surface area and micropore volume may have been due to errors associated with the porosity development, which are greater than the errors associated with the yield.

3.4.1. Porosity parameters and SEM of AC_{op}

Fig. 5a shows the N_2 adsorption and desorption isotherm for AC_{op}. The initial volume increased significantly with the relative pressure up to 0.6. According to the IUPAC, the N_2 adsorption curves are type I (reversible), indicating that AC_{op} is microporous.

Table 5
Optimum conditions given by the model and the model verification.

Activation temperature (°C), X_1	761.70
Activation time (h), X_2	0.86
Impregnation ratio (NaOH:char), X_3	3.46
BET surface area ($m^2\ g^{-1}$)	
Predicted	2589
Experimental ($n = 3$)	2854 ± 182
Micropore volume ($cm^3\ g^{-1}$)	
Predicted	1.27
Experimental ($n = 3$)	1.44 ± 0.07
Yield (%)	
Predicted	10.44
Experimental ($n = 3$)	10.80 ± 0.40

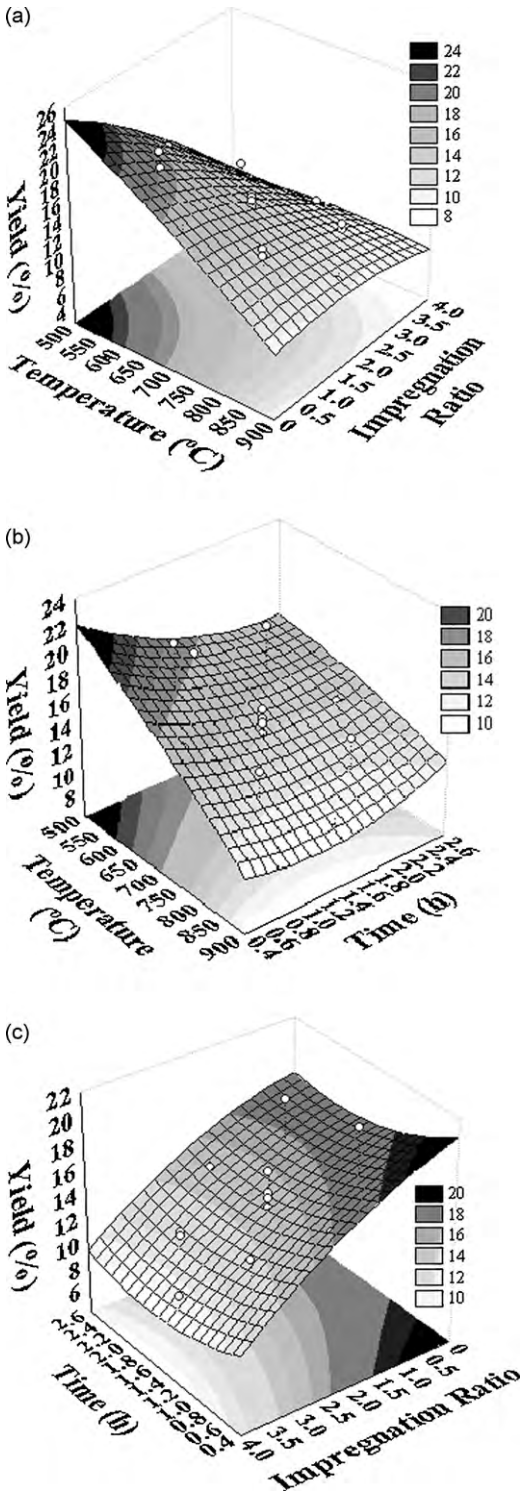

Fig. 4. Three-dimensional response surface plots for yield: impregnation ratio and temperature (a), time and temperature (b), and impregnation ratio and time (c).

Additionally, the plateau was practically parallel to the P/P^0-axis, confirming the presence of micropores with few mesopores [23]. The other properties of AC_{op} were: 1.60 $cm^3\ g^{-1}$, 0.16 $cm^3\ g^{-1}$, 90%, and 2.24 nm for the total pore volume, mesopore volume, percent micropores, and pore diameter, respectively. The predominance of micropores is evident, corresponding to 90% of the total, with only 10% of mesopores.

The pore size distribution of AC_{op} obtained by the HK method is shown in Fig. 5b. This method permits calculating the pore distribu-

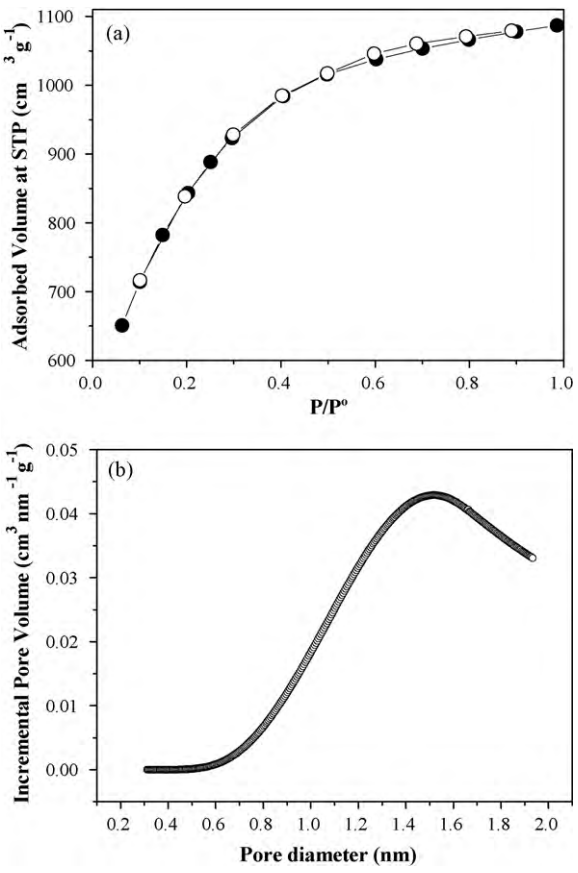

Fig. 5. N_2 Adsorption (●) and desorption (○) isotherms at 77 K (a) and pore size distribution (b) of AC_{op}.

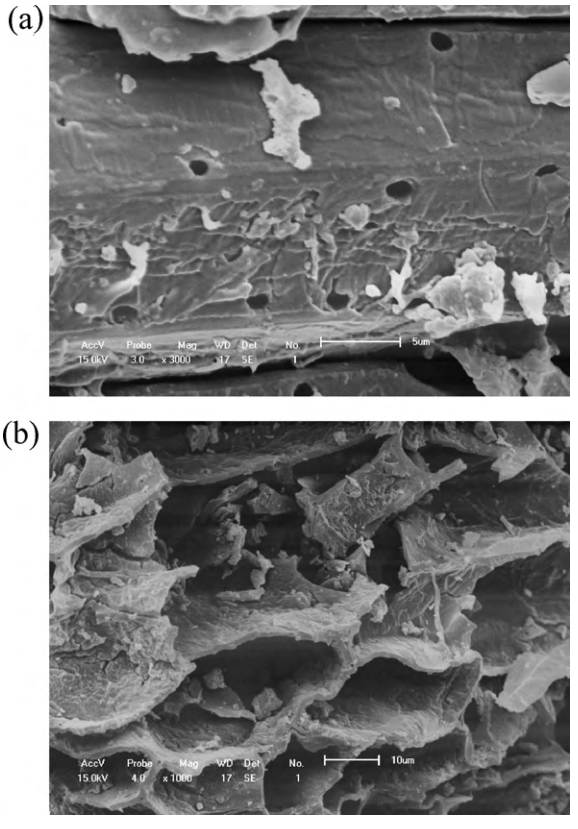

Fig. 6. Scanning electron micrographs of the raw material (a) and AC_{op} (b).

tion in the micropore region [24]. It is observed that the majority of pores have a diameter of 1.51 nm, corresponding to the secondary micropore region [11].

Fig. 6a and b shows the SEM images of the raw material and of AC_{op}, respectively. The formation of well-defined pores after the activation process can be observed.

4. Conclusions

The effects of three activated carbon preparation variables: activation temperature, activation time and impregnation ratio (NaOH:char), on the BET surface area, micropore volume and activated carbon yield were studied by conducting a central composite rotatable design (CCRD). Quadratic models were developed to correlate the preparation variables to the three responses.

According to the statistical model, the data were efficiently adjusted to the surface response models, and it was possible to evaluate the true relationship between the responses and the studied factors. The F ratio and p value indicate that the activation temperature and the impregnation ratio are the most important factors in the activation process. The increase in these factors favors the increase in the BET surface area and micropore volume. However, at the same time, reduces the AC yield.

The optimal activated carbon (AC_{op}) was obtained using activation temperature of 761.70 °C, activation time of 0.86 h, and impregnation ratio (NaOH:char) of 3.46. The AC_{op} showed BET surface area of 2854 $m^2\,g^{-1}$, micropore volume of 1.44 $cm^3\,g^{-1}$, and yield of 10.80%. The characteristics of the material (AC_{op}) obtained enable its application in gas adsorption.

Acknowledgements

The authors acknowledge COMCAP (Complexos de Centrais de Apoio à Pesquisa), Fundação Araucária and CAPES for the financial support.

References

[1] J. Alcañiz-Monge, D. Lozano-Castelló, D. Cazorla-Amorós, A. Linares-Solano, Fundamentals of methane adsorption in microporous carbons, Micropor. Mesopor. Mater. 124 (2009) 110–116.
[2] P. Nowicki, R. Pietrzak, H. Wachowska, Siberian anthracite as a precursor material for microporous activated carbons, Fuel 87 (2008) 2037–2040.
[3] D. Lozano-Castelló, J.M. Calo, D. Cazorla-Amorós, A. Linares-Solano, Carbon activation with KOH as explored by temperature programmed techniques, and the effects of hydrogen, Carbon 45 (2007) 2529–2536.
[4] J.A Mácia-Agulló, B.C. Moore, D. Cazorla-Amorós, A. Linares-Solano, Activation of coal tar pitch carbon fibres: physical activation vs. chemical activation, Carbon 42 (2004) 1367–1370.
[5] A.H. Basta, V. Fierro, H. El-Saied, A. Celzard, 2-Steps KOH activation of rice straw: an efficient method for preparing high-performance activated carbons, Bioresour. Technol. 100 (2009) 3941–3947.
[6] I.A.W. Tan, A.L. Ahmad, B.H. Hameed, Preparation of activated carbon from coconut husk: optimization study on removal of 2,4,6-trichlorophenol using response surface methodology, J. Hazard. Mater. 153 (2008) 709–717.
[7] I.A.W. Tan, A.L. Ahmad, B.H. Hameed, Optimization of preparation conditions for activated carbons from coconut husk using response surface methodology, Chem. Eng. J. 137 (2008) 462–470.
[8] C. Michailof, G.G. Stavropoulos, C. Panayiotou, Enhanced adsorption of phenolic compounds, commonly encountered in olive mill wastewaters, on olive husk derived activated carbons, Bioresour. Technol. 99 (2008) 6400–6408.
[9] M.A Lillo-Ródenas, A. Ros, E. Fuente, M.A. Montes-Morán, M.J. Martin, A. Linares-Solano, Further insights into the activation process of sewage sludge-based precursors by alkaline hydroxides, Chem. Eng. J. 142 (2008) 168–174.
[10] T. Kawano, M. Kubota, M.S. Onyango, F. Watanabe, H. Matsuda, Preparation of activated carbon from petroleum coke by KOH chemical activation for adsorption heat pump, Appl. Therm. Eng. 28 (2008) 865–871.
[11] J.V. Nabais, P. Carrott, M.M.L. Ribeiro Carrott, V. Luz, A.L. Ortiz, Influence of preparation conditions in the textural and chemical properties of activated carbons from a novel biomass precursor: the coffee endocarp, Bioresour. Technol. 99 (2008) 7224–7231.
[12] A.A. El-Hendawy, A.J. Alexander, R.J. Andrews, G. Forrest, Effects of activation schemes on porous, surface and thermal properties of activated carbons prepared from cotton stalks, J. Anal. Appl. Pyrol. 82 (2008) 272–278.
[13] R.L. Tseng, Physical and chemical properties and adsorption type of activated carbon prepared from plum kernels by NaOH activation, J. Hazard. Mater. 147 (2007) 1020–1027.
[14] F.C. Wu, R.L. Tseng, R.S. Juang, Preparation of highly microporous carbons from fir wood by KOH activation for adsorption of dyes and phenols from water, Sep. Purif. Technol. 47 (2005) 10–19.
[15] F.C. Wu, R.L. Tseng, High adsorption capacity NaOH-activated carbon for dye removal from aqueous solution, J. Hazard. Mater. 152 (2008) 1256–1267.
[16] R. Ubago-Pérez, F. Carrasco-Marín, D. Fairén-Jiménez, C. Moreno-Castilla, Granular and monolithic activated carbons from KOH-activation of olive stones, Micropor. Mesopor. Mater. 92 (2006) 64–70.
[17] M.A. Bezerra, R.E. Santelli, E.P. Oliveira, L.S. Villar, L.A. Escaleira, Response surface methodology (RSM) as a tool for optimization in analytical, Talanta 76 (2008) 965–977.
[18] D.C. Montgomery, Design and Analysis of Experiments, 5th ed., John Wiley & Sons, New York, 2001.
[19] R.H. Myers, D.C. Montgomery, Response Surface Methodology—Process and Product Optimization Using Designed Experiments, 1st ed., John Wiley & Sons, New York, 1995.
[20] B.H. Hameed, I.A.W. Tan, A.L. Ahmad, Preparation of oil palm empty fruit bunch-based activated carbon for removal of 2,4,6-trichlorophenol: optimization using response surface methodology, J. Hazard. Mater. 164 (2009) 1316–1324.
[21] B.H. Hameed, I.A.W. Tan, A.L. Ahmad, Optimization of basic dye removal by oil palm fibre-based activated carbon using response surface methodology, J. Hazard. Mater. 158 (2008) 324–332.
[22] ASTM D1762-84. Annual book of ASTM standards D1762-84 (1984) pp. 292–293.
[23] K.S.W. Sing, D.H. Everett, R.A.W. Haul, L. Moscou, R.A. Pierotti, J. Rouquérol, T. Siemieniewska, Reporting physisorption data for gas/solid systems with special reference to the determination of surface area and porosity, Pure Appl. Chem. 57 (1985) 603–619.
[24] R.J. Dombrowski, C.M. Lastoskie, D.R. Hyduke, The Horvath–Kawazoe method revisited, Colloids Surf. A 187–188 (2001) 23–39.
[25] G. Derringer, R. Suich, Simultaneous Optimization of Several Response Variables, J. Qual. Technol. 12 (1980) 214–219.